

Moiré Potential, Lattice Corrugation, and Band Gap Spatial Variation in a MoTe₂/MoS₂ Heterobilayer

W. T. Geng¹, V. Wang,² Y. C. Liu,^{2,1} Takahisa Ohno,¹ and Jun Nara¹

¹ National Institute for Materials Science, Tsukuba 305-0044, Japan
Phone: +81-70-4486-3271 E-mail: geng.wentong@nims.go.jp

² Xi'an University of Technology, Xi'an 710054, China

Abstract

we have performed first-principles calculations on a MoTe₂(9×9)/MoS₂(10×10) stacking. Lattice corrugation is found to be significant in both monolayers, yet its effect on the electronic properties is marginal. The variation of the average local potential near Mo atoms in both MoTe₂ and MoS₂ layers displays a conspicuous Moiré pattern, correlating closely with the spatial variation of the valence band maximum and conduction band minimum, and thus can be taken as the intralayer Moiré potential. The interlayer Moiré potential, defined as the difference between the two intralayer Moiré potentials, changes roughly in proportion to the band gap variation in the Moiré cell.

1. Introduction

Moiré pattern in van der Waals (vdW) bilayers a rich source in generating new quantum phenomena. [1] Moiré potential describes the spatial variation of the potential within a Moiré cell. MacDonald's group are the first to evaluate the Moiré potential of vdW bilayers, making use of information obtained from density functional theory (DFT) calculations on high-symmetry local crystalline structures without mismatch and twist to derive effective Hamiltonians that are able to efficiently describe the effect of the moiré pattern on electronic properties of the long-period superlattices. [2] If the constituent monolayers differ much in lattice constants, such as in the transition metal dichalcogenide (TMDC) bilayer having different chalcogen elements, this effective model will not be applicable because strain has strong influence on the electronic structures. Besides, the Moiré potential defined this way is only available after the band gap of the Moiré cell has been determined. Since strain has strong influence on the electronic structures of TMDC, full DFT treatment is highly desirable in order to get more precise details of the Moiré potential which determines the lattice corrugation of the bilayer, the spatial variation of the band gap, and many other quantum phenomena arising from interlayer vdW interactions.

2. Computational Methods

The DFT computation was performed using Vienna Ab initio Simulation Package.[4] The electron-ion interaction was described using projector augmented wave method. The exchange correlation between electrons was treated both with generalized gradient approximation in the Perdew-Burke-Ernzerhof form. The non-bonding vdW interaction was incorporated by employing a semi-empirical correction scheme of Grimme's DFT-D3 method. [5] We used an energy cutoff of

400 eV for the plane wave basis set for all systems, both monolayers and bilayers, to ensure equal footing. The Brillouin-zone integration was performed within Monkhorst-Pack scheme using k meshes of (12×12×1) for (1×1) monolayer unit cells and (1×1×1) (Γ point only) for MoTe₂(9×9)/MoS₂(10×10) stacking. A finer k -mesh of (551) was used for the density of state. Due to the extremely heavy weight of computation for such a large supercell, spin-orbit coupling was not taken into account.

3. Results, discussion, and conclusions

Fig. 1A shows top view of the heterobilayer. In the side view (Fig. 1B), lattice corrugation is clearly seen.

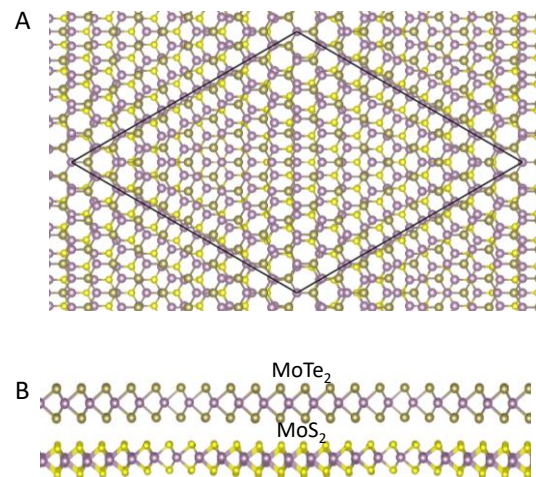


Fig. 1 Geometry of MoTe₂/MoS₂ bilayer.

The calculated band structures of the heterobilayer near the Fermi level (set to zero), with (panel A) and without out-of-plane relaxation (pane B) are plotted in Fig. 2. It is seen that corrugation influences the band structure only marginally, due to the weakness of vdW interactions. The VBM shifts down from -0.256 to -0.258eV, the CBM shifts up from 0.584 to 0.585eV, and the band gap increases from 0.840 to 0.843eV. The valence band is mainly contributed by 4*d* orbitals of Mo_{Tc} and partially by 5*p* states of Te. The conduction band consists of mainly 4*d* of Mo_S and the contribution from 3*p* states of S is insignificant. The VBM appears at the Γ point, which corresponds to the K point in the unfolded Brillouin zone of a free-standing MoTe₂ monolayer, and the CBM is located at the K point, corresponding also to the K point of a free-standing MoS₂ monolayer.

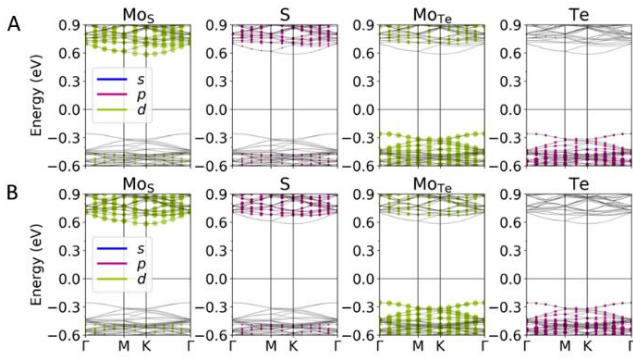


Fig. 2 Species-projected band structure of the heterobilayer $\text{MoTe}_2(9 \times 9)/\text{MoS}_2(10 \times 10)$ with (A) and without (B) out-of-layer relaxation.

We turn to the density of states (DOS) localized in a particular atom to obtain the its distribution in energy space, which fulfills our need for knowledge of band gap variation (Fig. 3A). To make the displacement of LDOS curves more visible, we follow Carr et al. [3] in making use of the logarithm of LDOS (bottom panel) to estimate VBM and CBM for a selected number of Mo atoms (Fig. 3B). We find that the VBM varies much less strongly within the Moiré cell than does CBM. This is in accordance with the fact that MoTe_2 layer has dielectric constants about four times as large as that of MoS_2 , thus it is less susceptible to the electric field produced by Moiré pattern. Another finding is that the change of VBM has an opposite sign to that of CBM. With the knowledge of VBM and CBM for different Mo atoms, we can readily obtain the spatial variation of band gap in the Moiré cell.

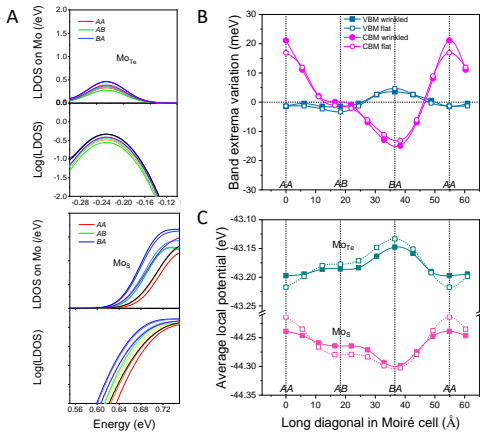


Fig. 3 (A) DOS of the heterobilayer. (B) Variation of the VBM and CBM with and without out-of-layer geometry relaxation. (C) The average local potential at the MoTe_e and MoS_s atoms.

Since a bilayer TMDC heterostructure is not strictly a 2D system, but rather composed of six atomic layers in the vertical direction, the definition of Moiré potential in real space, which is essentially a 2D function, depends on the surface or curved surface on which the phenomenon under investigation is present. Having realized that the valence and conduction bands are contributed mainly by MoTe_e and MoS_s atomic layer,

respectively, we now examine the variation of the total local potential at the MoTe_e and MoS_s atoms. We argue that it is neither feasible nor necessary to trace the change of local potential at every single point in the primitive unit cell, a good representation could be the average of the local potential around the sole Mo atom therein. We plot in Fig. 3C the calculated average local potential at the MoTe_e and MoS_s atoms. The data points, when connected with spline lines, forming an envelope curve that indicates the amplitude of the local potential modulation. We can define the intralayer Moiré potential of the valence or conduction band as the variation of the corresponding average local potential in reference to its average over the Moiré cell. The interlayer Moiré potential which relates to the band gap, can therefore be defined as the difference between the two intralayer Moiré potentials.

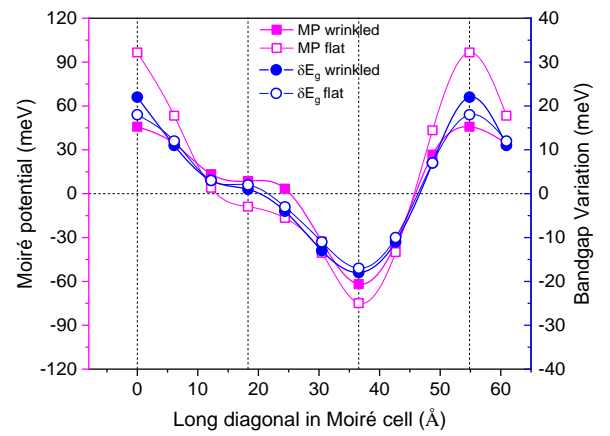


Fig. 4 Correlation of the Moiré potential (squares) and bandgap variation (circles) in a $\text{MoTe}_2(9 \times 9)/\text{MoS}_2(10 \times 10)$ bilayer with (solid symbols) and without (empty symbols) out-of-layer geometry relaxation. Data points are connected by spline lines to guide the eye.

In Fig. 4, it is found that corrugation reduces remarkably the amplitude of the Moiré potential, from 0.17 to 0.11 eV. The change of band gap along the long diagonal of the Moiré cell has an amplitude of 0.04 eV. In contrast to its effect on the Moiré potential, lattice corrugation of the bilayer enhances the spatial variation of the local band gap by 5 meV. On the other hand, its influence on the global band gap is within 1 meV.

Acknowledgements

This work was supported by Innovative Science and Technology Initiative for Security Grant Number JPJ004596, ATLA, Japan. The calculations were carried out on Numerical Materials Simulator of NIMS.

References

- [1] Y. Cao et al., *Nature* **556** (2018) 43.
- [2] J. Jung et al. *Phys. Rev. B* **89** (2014) 205414.
- [3] G. Kresse and J. Furthmuller, *Phys. Rev. B* **54** (1996) 11169.
- [4] J. Klimeš, D. R. Bowler, A. Michaelides, *Phys. Rev. B* **83** (2011) 195131.
- [5] S. Carr et al. *Phys. Rev. B* **95** (2017) 075420.